ACS SENSORS

pubs.acs.org/acssensors Article

Simultaneous Dopamine and Serotonin Monitoring in Freely Moving Crayfish Using a Wireless Electrochemical Sensing System

Jinjing Han,[#] Ta-wen Ho,[#] Justin M. Stine, Sydney N. Overton, Jens Herberholz, and Reza Ghodssi*

Cite This: https://doi.org/10.1021/acssensors.3c02304 Read Online

ACCESS | Metrics & More | Article Recommendations | Supporting Information

ABSTRACT: Dopamine (DA) and serotonin (5-HT) are neurotransmitters that regulate a wide range of physiological and behavioral processes. Monitoring of both neurotransmitters with real-time analysis offers important insight into the mechanisms that shape animal behavior. However, bioelectronic tools to simultaneously monitor DA and 5-HT interactive dynamics in freely moving animals are underdeveloped. This is mainly due to the limited sensor sensitivity with miniaturized electronics. Here, we present a semi-implantable electrochemical device achieved by integrating a multi-surface-modified carbon fiber microelectrode with a miniaturized potentiostat module to detect DA and 5-HT in vivo with high sensitivity and selectivity. Specifically, carbon fiber microelectrodes were modified through electrochemical treatment and surface coatings to improve sensitivity, selectivity, and antifouling properties. A customized, lightweight potentiostat module was developed for untethered electrochemical measurements. Integrated with the microelectrode, the microsystem is compact (2.8 × 2.3 × 2.1 cm) to minimize its impacts on animal behavior and achieved simultaneous detection of DA and 5-HT with sensitivities of 48.4 and 133.0 nA/μM, respectively, within submicromolar ranges. The system was attached to the crayfish dorsal carapace, allowing electrode implantation into the heart of a crayfish to monitor DA and 5-HT dynamics, followed by drug injections. The semi-implantable biosensor system displayed a significant increase in oxidation peak currents after DA and 5-HT injections. The device successfully demonstrated the application for in vivo simultaneous monitoring of DA and 5-HT in the hemolymph (i.e., blood) of freely behaving crayfish underwater, yielding a valuable experimental tool to expand our understanding of the comodulation of DA and 5-HT.

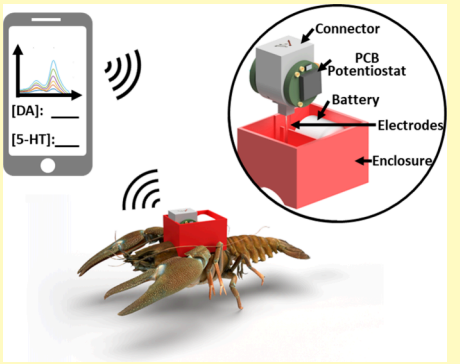

KEYWORDS: *serotonin, dopamine, biosensing, electrochemistry, implantable, in vivo, freely moving animal, wireless system*

Monoamine neurotransmitters, such as dopamine (DA) and serotonin (5-HT), have been implicated in a wide range of physiological and behavioral processes in animals. DA is well-known for regulation of reward and motivational action,[1−3] while 5-HT has diverse functions in modulating behavioral states, spanning from locomotor activity to feeding, sleep and arousal states, mood regulation, and higher order cognition.[4] Multiple studies have demonstrated involvement of both DA and 5-HT in regulating social behaviors in crustaceans and other animals, more specifically, aggression, motivation to engage in agonistic encounters, and social hierarchy formation and maintenance.[5−8] Therefore, the codetection of DA and 5-HT in animals would help in understanding the mechanisms underlying their combined effects in modulating social behaviors.

Existing methods for quantifying neurochemical *in vivo* include various approaches such as tethered microdialysis probes,[9,10] optical fibers,[11,12] and electrochemical sensors.[13−15] These methods have been instrumental in advancing our understanding of neurobiology, psychopharmacology, and behavioral neuroscience, revealing new insights into phenomena like the sleep−wake cycle[10] and reward-related response.[16] Behavioral assays usually involve confining a single animal within a box or cylinder with an open top. During *in vivo* experiments, guide cannulas, optical fibers, electrodes, and other components are typically affixed to the animal's skull, allowing for direct connection of electrical cables and fluid lines.[17−19] However, these wires are intrusive and often restrain the animals. Freely behaving animals may coil or damage the wires. Furthermore, wires limit the animals' range and hinder experiments exploring interactions between multiple animals. Despite the strong desire to develop wirelessly operated devices for detecting neurotransmitters in living animals, this area of research remains a major challenge.

Crayfish present an ideal model system to investigate the neurochemistry underlying neurobehavioral changes, as their behaviors are well-characterized and quantifiable. In crayfish, injections of 5-HT into the circulatory system (hemolymph)

Received: October 30, 2023
Revised: April 17, 2024
Accepted: April 22, 2024

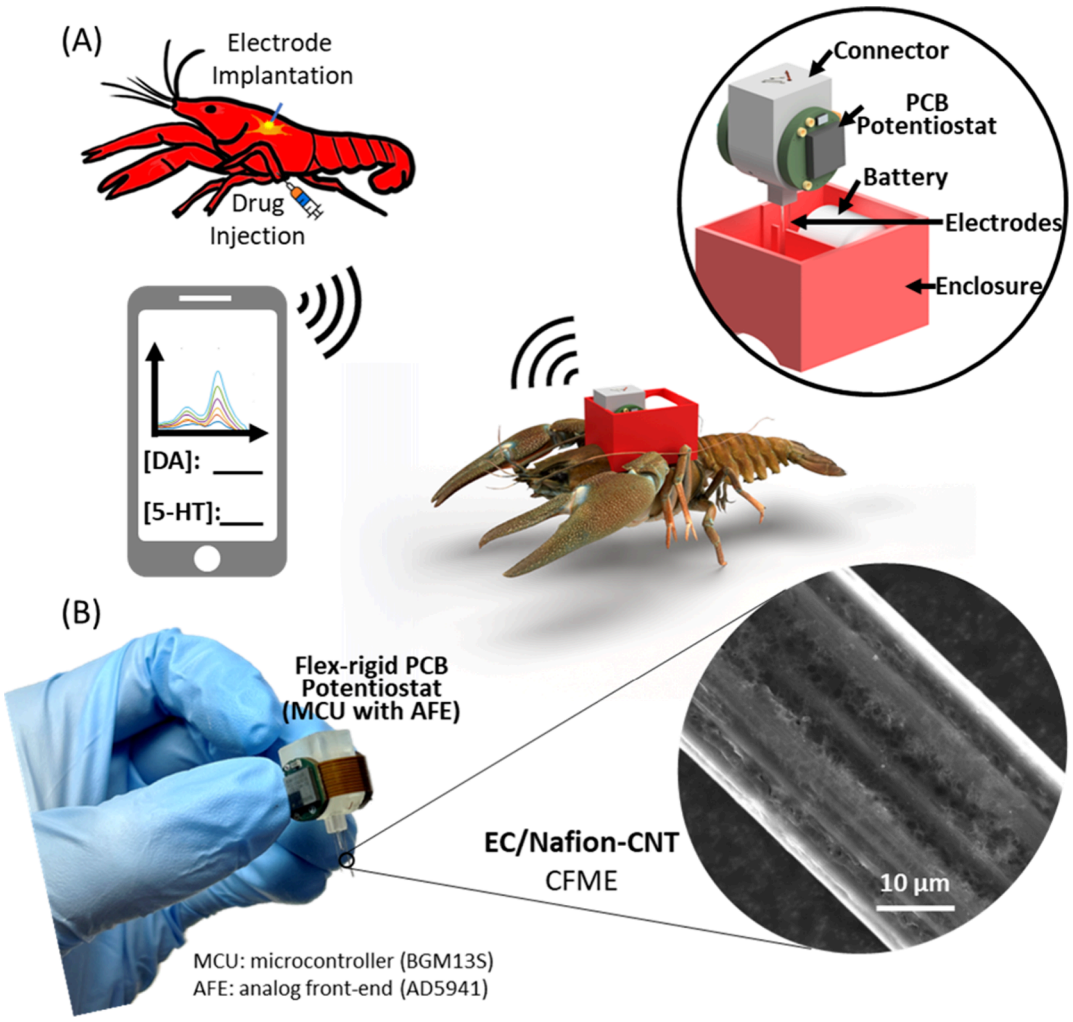

Figure 1. (A) Schematic illustrations depict the electrochemical sensing device and its capabilities for wireless simultaneous detection of DA and 5-HT. The CFME is implanted in the heart of a crayfish, while the drug is injected into the crayfish's ventral sinus cavity. (B) Photograph showing the integrated device hardware with a customized PCB, a 3D printed connector, and implantable electrodes. An SEM image of the CFME shows the surface-modified EC/Nafion-CNT CFME.

can promote aggression and anxiety-like behavior.[20−23] However, injections of DA resulted in an opposing effect on agonistic and phototactic behaviors as those seen with 5-HT.[24,25] The underlying mechanisms remain poorly understood and require further investigation. One reason for this critical gap in knowledge is the lack of miniaturized technology to achieve wireless monitoring of neurotransmitter dynamics with real-time analysis in freely behaving animals.

Previously, we demonstrated surface-modified carbon fiber microelectrodes (CFMEs) for 5-HT sensing with improved sensitivity, selectivity, and fouling resistance.[26] The CFMEs were coated with Nafion, a negatively charged, perfluorinated ion-exchange film, showing improved selectivity for cationic amines, such as 5-HT, over negatively charged interference molecules like uric acid (UA), ascorbic acid (AA), 5-HT metabolite—5-hydroxyindoleacetic acid (5-HIAA)—and DA metabolite—3,4-dihydroxyphenylacetic acid (DOPAC)—during electrostatic interaction.[27−30] Electrochemical treatment, which was achieved by applying repeated cyclic voltammetry (CV) cycles, and carbon nanotube (CNT) coating have demonstrated improved sensitivity and antifouling properties due to induced nanostructure, functional groups, and increased surface area.[26,31] The developed microelectrode was also applied for *in vivo* 5-HT sensing with a wired connection in crayfish.[32,33]

The prior work still bears the following challenges: (a) limited microelectrode repeatability for *in vivo* measurement due to its fragility and (b) restricted animal movement due to wired connections. To address these limitations, the current work reports on a wireless electrochemical sensing device with novel surface modified CFME for simultaneous monitoring of DA and 5-HT in freely moving crayfish. The untethered semi-implantable system features a robust multifiber CFME interfaced with a miniaturized potentiostat module for wireless control and data acquisition via Bluetooth connection. Our device enables simultaneous monitoring of DA and 5-HT dynamics *in vivo* and underwater through CV measurements in the hemolymph without affecting crayfish behavior during operation. This work provides a potential engineering approach to facilitate a better understanding of the impact of dopaminergic and serotonergic modulation on animal behaviors.

RESULTS AND DISCUSSION

Overall Design of the System. The overall wireless electrochemical DA and 5-HT monitoring system consisted of

https://doi.org/10.1021/acssensors.3c02304
ACS Sens. XXXX, XXX, XXX−XXX

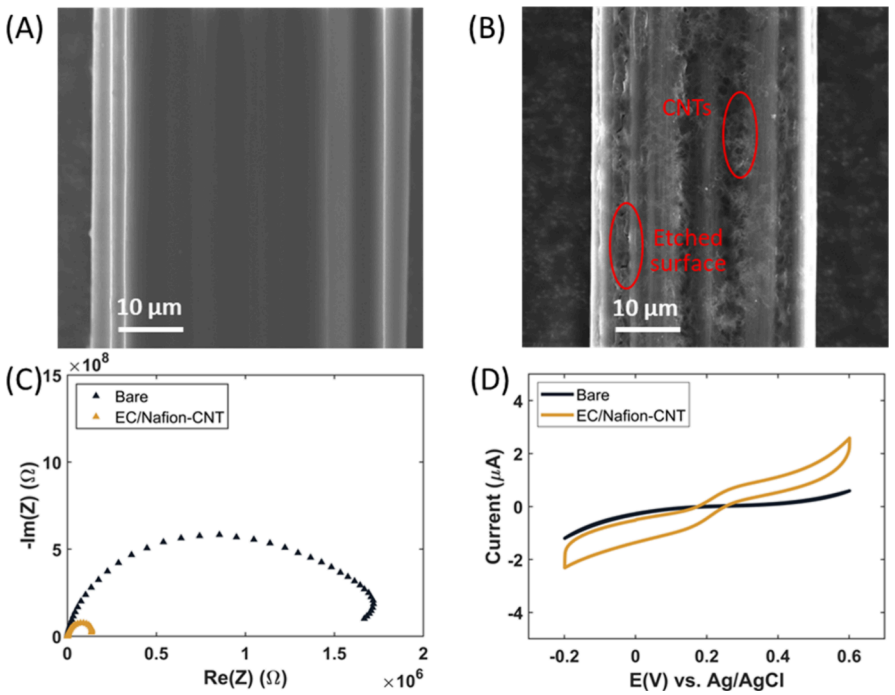

Figure 2. Surface characterization of CFMEs. SEM images of (A) bare and (B) EC/Nafion-CNT CFMEs. (C) Nyquist plot for bare and EC/Nafion-CNT CFMEs in 0.1 M KCl with 10 mM $[Fe(CN)_6]^{3-}/[Fe(CN)_6]^{4-}$ solution, within a frequency range of 0.1 to 1 MHz. (D) CV curves of bare and EC/Nafion-CNT CFMEs in 0.1 M KCl with a 10 mM $[Fe(CN)_6]^{3-}/[Fe(CN)_6]^{4-}$ solution. The potential ranges from −0.1 to 0.6 V with a scan rate of 100 mV/s.

a customized three-electrode configuration, a flexible-rigid printed circuit board (PCB) potentiostat module, and a 3D printed package (Figure 1). The 3D printed package was composed of two components: (i) an alignment connector printed with clear resin using digital light processing (DLP) (M50, CADWorks3D) to hold the electrodes and provide electrical connections between the electrodes and the PCB potentiostat and (ii) an enclosure printed with polylactic acid (PLA) using fused filament fabrication (FFF) (MK3S+, Prusa) to provide an interface with the crayfish. A small cutout (3 × 3 mm) on the enclosure allowed the sensor electrodes to access the attached crayfish. The entire waterproof device was powered by a single 3 V coin cell lithium battery (2L76, Energizer, USA) and was capable of monitoring DA and 5-HT levels in freely behaving crayfish underwater while wirelessly transmitting the data to a smartphone.

Fabrication and Characterization of Electrodes. Previously, we have shown electrochemical treatment effectively increased electrochemical active surface area than nontreatment samples. Increased defect sites/edge plane sites and increased oxygen element content in the treated carbon fiber samples also contribute to improved electrochemical performance and sensing capability toward 5-HT.[32,33] Here, the surface morphology of the surface-modified CFME was characterized by scanning electron microscopy (SEM). As shown in Figure 2A,B, the bare carbon fibers exhibit a smooth surface with striations, which is typical of carbon fibers produced through the polyacrylonitrile (PAN) manufacturing process. However, after undergoing surface modifications including electrochemical treatment and Nafion-CNT coating, the EC/Nafion-CNT surface becomes rougher with a dense coating of carbon nanotubes (CNTs). The energy-dispersive X-ray spectroscopy (EDS) analysis (Figure S2) confirms the presence of fluorine on the surface, likely due to the Nafion ($C_7HF_{13}O_5S{\cdot}C_2F_4$) coating.

The effect of electrochemical treatment and surface coating of the Nafion-CNT thin film was investigated using electrochemical impedance spectroscopy (EIS) and CV measurements with a 10 mM $[Fe(CN)_6]^{3-}/[Fe(CN)_6]^{4-}$ solution (Figure 2C,D. Figure 2C displays the EIS spectra of the samples, confirming that the EC/Nafion-CNT electrode exhibits a higher conductivity compared to the bare electrode. This suggests that the treatment enhances the ionic transport between the electrolyte and active material, thereby facilitating greater electrochemical redox activity. This finding is consistent with the CV result, where no visible peaks were observed for the bare electrode, indicating that the electrochemical oxidation and reduction of ferricyanide and ferrocyanide do not readily occur on the bare CFME (Figure 2D). In contrast, the CV curve for the EC/Nafion-CNT electrode shows substantially larger current output, indicating faster electron-transfer reactions.[34] It should be noted that the Nafion-CNT thin film has been reported to improve the selectivity[28] and possess fouling resistance.[31] In conclusion, the electrochemically treated electrodes exhibit reduced electron transfer resistance, leading to enhanced electrochemical redox activity.

Analytical Performance of EC/Nafion-CNT CFMEs. The surface-modified electrode for DA and 5-HT sensing was studied and is represented in Figure 3. The EC/Nafion-CNT electrode exhibits oxidation peak potentials (Epas) of 0.23 V for DA and 0.4 V for 5-HT, respectively. The oxidation peak currents (Ipas) of these analytes increased linearly with increasing concentrations. CV responses of the EC/Nafion-CNT CFME to DA and 5-HT are shown in Figure 3A−C, with the calibration curved plotted in Figure 3D−F.

https://doi.org/10.1021/acssensors.3c02304
ACS Sens. XXXX, XXX, XXX−XXX

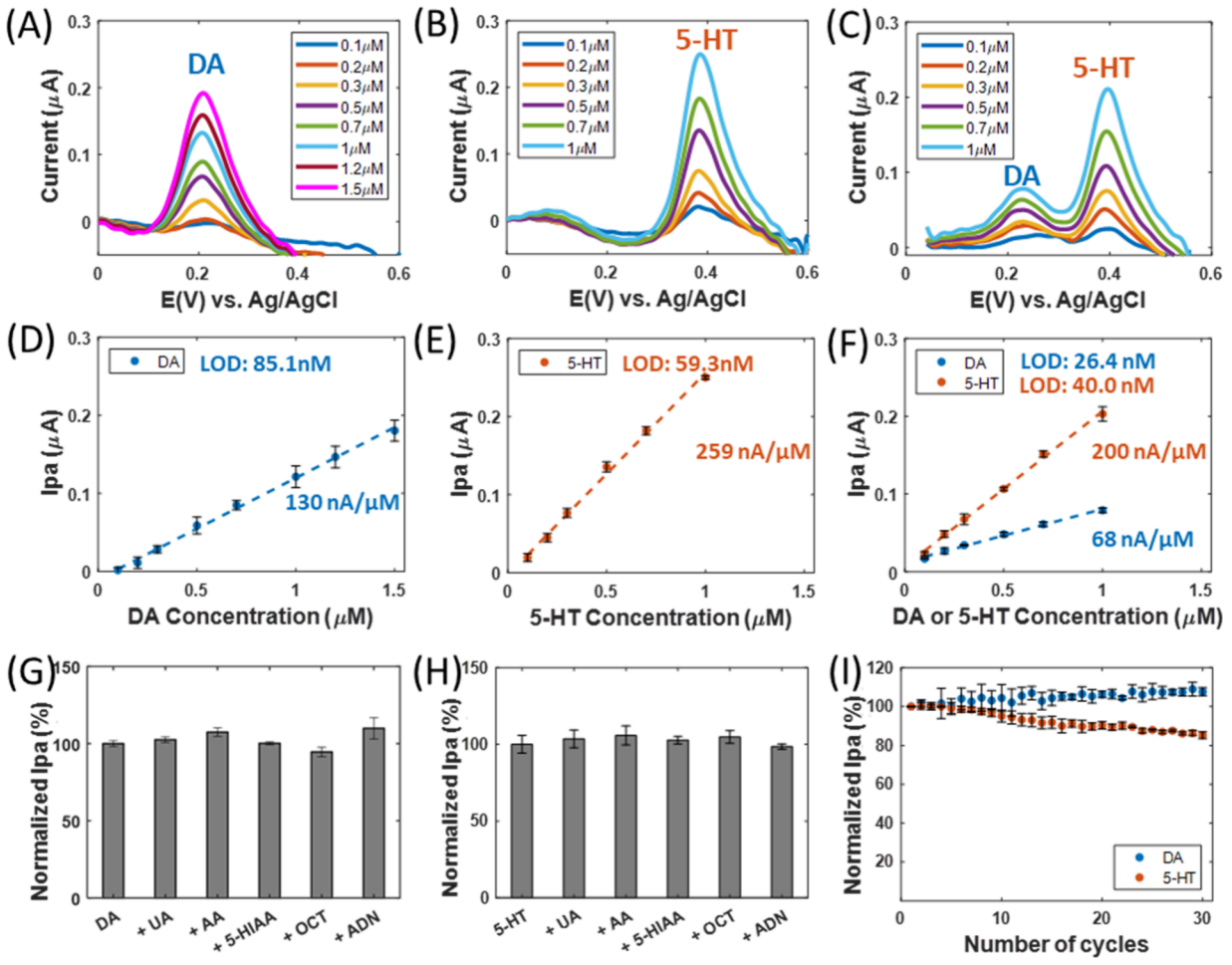

Figure 3. Analytical performance of the EC/Nafion-CNT CFME for DA and 5-HT detection. Background-subtracted voltammetric response of the CFME with (A) DA concentrations ranging from 0.1 to 1.5 μM in 1X PBS; (B) 5-HT concentrations ranging from 0.1 to 1 μM in 1X PBS; and (C) equimolar mixture of DA and 5-HT concentrations ranging from 0.1 to 1 μM in 1× PBS. Calibration curve of (D) DA concentrations ranging from 0.1 to 1.5 μM in 1× PBS (R^2 = 0.9974); (E) 5-HT concentrations ranging from 0.1 to 1 μM in 1× PBS (R^2 = 0.9959); and (F) equimolar mixture of DA (R^2 = 0.9947) and 5-HT (R^2 = 0.9977) concentrations ranging from 0.1 to 1 μM in 1× PBS. (G) Interference response of the EC/Nafion-CNT for the detection of 1 μM DA in the presence of 20 μM UA, AA, 5-HIAA, OCT, and ADN. The Ipas are normalized to 1 μM DA (n = 3). (H) Interference response of the EC/Nafion-CNT for the detection of 1 μM 5-HT in the presence of 20 μM UA, AA, 5-HIAA, OCT, and ADN. The Ipas are normalized to 1 μM 5-HT (n = 3). (I) Ipas of the EC/Nafion-CNT recorded in 1 μM DA or 1 μM 5-HT over 30 consecutive measurements. The Ipas are normalized to the value for the initial cycle (n = 3).

The CV responses of EC/Nafion-CNT CFMEs to DA are shown in Figure 3A. The calibration curve, plotted in Figure 3D, demonstrates that the CV currents of DA exhibit linear relationships with the DA concentration ranging from 0.1 to 1.5 μM. The sensitivity is calculated to be 130 nA/μM with a standard error (σ) of 3.68 nA and a limit of detection (LOD) of 85.1 nM. Figure 3B illustrates the voltammetric responses of the sensor to 5-HT concentrations in the range of 0.1 to 1 μM. The sensor exhibits a linear response to 5-HT concentrations in this range, with a sensitivity of 259 nA/μM and a LOD of 59.3 nM, with a σ of 5.12 nA (Figure 3E). Furthermore, the EC/Nafion-CNT electrode was also tested for simultaneous detection of DA and 5-HT (Figure 3C). Two well-defined oxidation peaks were observed, and their Epas remained unchanged. The Ipas of DA and 5-HT increased linearly with their concentrations in the range of 0.1 to 1 μM. The sensitivity of DA and 5-HT were calculated to be 68 and 200 nA/μM, respectively. The LOD of DA and 5-HT were calculated to be 26.4 (with σ = 0.60 nA) and 40.0 nM (with σ = 2.66 nA), respectively (Figure 3F). It is evident that simultaneous DA and 5-HT measurements were achieved on the EC/Nafion-CNT with high sensitivity.

During the simultaneous detection of DA and 5-HT, a decrease was observed in both sensitivity and LOD compared to the individual detection of DA and 5-HT. This phenomenon is likely attributed to a competitive binding scenario between DA and 5-HT for the finite binding sites on the electrode surface.[35,36] Given the structural similarity of DA and 5-HT, characterized by their benzene ring structure, their interactions vie for the same limited binding sites on the electrode surface, thereby leading to a diminished signal response.

To explore the selectivity of the sensor between DA, 5-HT, and other potential interfering molecules in crayfish, CV measurements of 1 μM DA (Figure S3) and 1 μM 5-HT (Figure S4) were performed in the absence and presence of 20 μM UA, AA, 5-HIAA, octopamine (OCT), and adenosine (ADN). The results demonstrate that even at a 20-fold concentration of UA, AA, 5-HIAA, OCT, and ADN, the accurate detection of DA and 5-HT remained largely

https://doi.org/10.1021/acssensors.3c02304
ACS Sens. XXXX, XXX, XXX−XXX

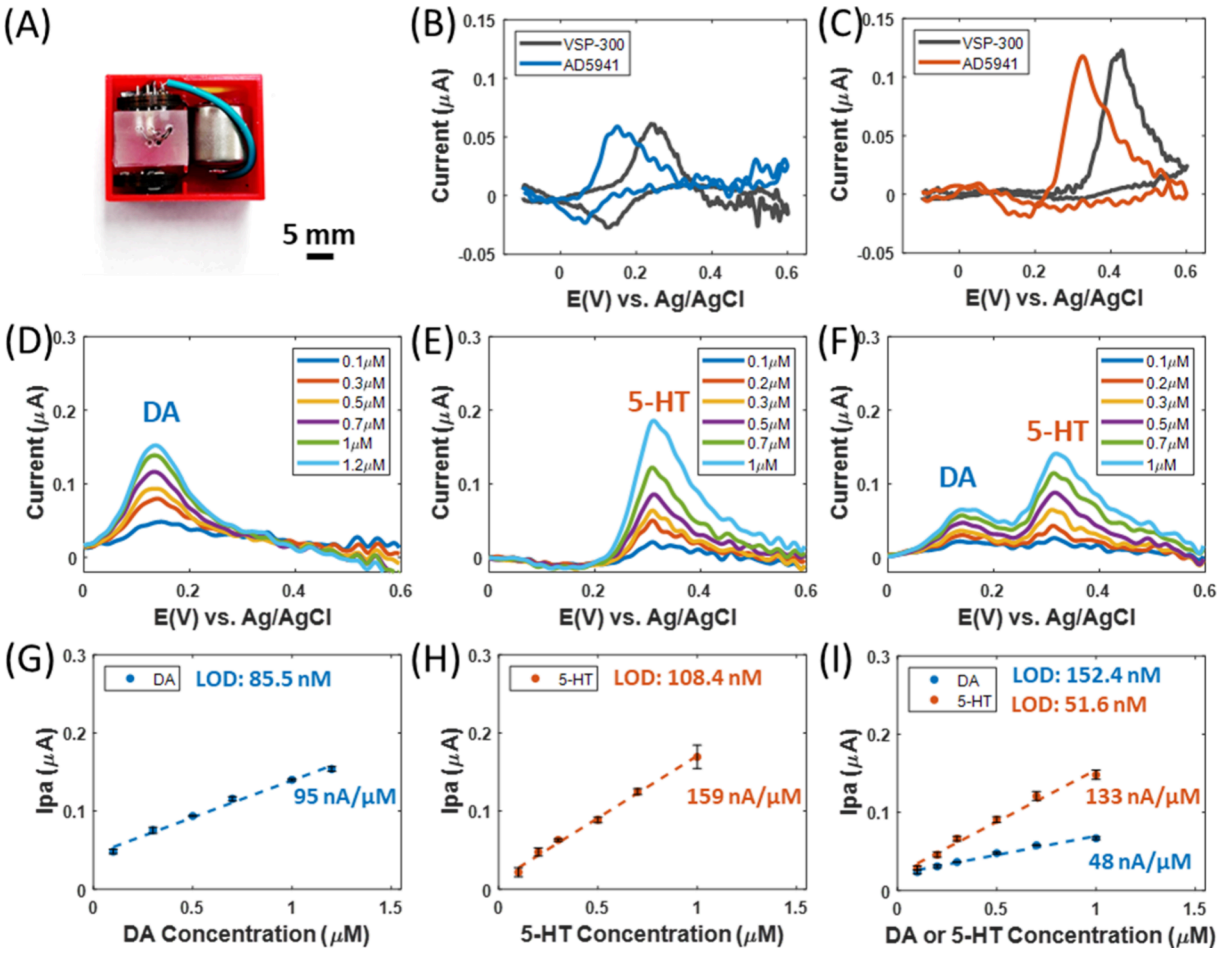

Figure 4. Analytical performance of the wireless neurotransmitter sensing device for DA and 5-HT detection. (A) Image of the system. Background-subtracted cyclic voltammogram comparing the benchtop potentiostat and the electrochemical sensing system in (B) 1 μM DA and (C) 1 μM 5-HT. Potential range: −0.1 to 0.6 V. Scan rate: 100 mV/s. Background-subtracted voltammetric response and calibration curve of the sensing system with (D) DA concentrations of 0.1 to 1.2 μM in 1× PBS, (E) 5-HT concentrations of 0.1 to 1 μM in 1× PBS, and (F) equimolar mixture of DA and 5-HT concentrations of 0.1 to 1 μM in 1× PBS. Calibration curve of (G) DA with concentrations of 0.1 to 1.2 μM (R^2 = 0.9890), (H) 5-HT with concentrations of 0.1 to 1 μM (R^2 = 0.9943), and (I) equimolar mixture of DA (R^2 = 0.9804) and 5-HT (R^2 = 0.9853) with concentrations of 0.1 to 1.0 μM.

unaffected (Figure 3G,H). The observed differences were minimal, with less than a 10% variation compared with the control measurements. These findings indicate that the presence of higher concentrations of UA, AA, 5-HIAA, OCT, and ADN did not significantly interfere with the accurate detection and quantification of DA and 5-HT.

To assess the potential applicability of the developed electrode in animal models other than crayfish, we examined the selectivity between norepinephrine (NE) and DA (Figure S3F) as well as between histamine (HA) and 5-HT (Figure S4F). Our findings revealed minimal interference between 5-HT and HA, with only a 5.2% increase observed with the addition of 20 μM HA to 1 μM 5-HT. However, NE did interfere with DA detection, resulting in a 22.6% increase in current response when an additional 20 μM NE was introduced to 1 μM DA. These results underscore the importance of carefully selecting the animal model and area of interest for electrode implantation.

The stability of the CFME was assessed by recording the response currents of the electrode in 1 μM DA or 5-HT for 30 continuous cycles at a rate of 1 cycle/min (Figure 3I). The results indicated that after 30 cycles, the current responses for DA and 5-HT were 107 and 85% of the initial current response, respectively.

Overall, the results demonstrate the promising potential of the EC/Nafion-CNT CFMEs for continuous and simultaneous detection of DA and 5-HT, given their high sensitivity, selectivity, and repeatability.

Analytical Performance of Integrated Electrochemical Sensing System. The sensitivity of the fully integrated electrochemical sensing system was characterized. The overall system design was compact (Figure 4A) with dimensions of 28 × 23 × 21 mm, consisting of a customized three-electrode system, a PCB potentiostat, and a battery. To evaluate its electrochemical performance, the electrochemical system was compared to a benchtop potentiostat with a standard RE/CE. CV responses of the electrochemical device to DA and 5-HT in PBS were recorded on the phone application through BLE wireless data transmission and plotted in MATLAB. Figure 4B compares the cyclic voltammograms of 1 μM DA that were recorded using a commercial benchtop potentiostat (VSP-300) and our device (AD5941). The Epas for DA were observed to be 0.24 V using VSP-300, compared to 0.15 V recorded by the integrated system. The Ipas were measured to be 60 nA for

https://doi.org/10.1021/acssensors.3c02304
ACS Sens. XXXX, XXX, XXX−XXX

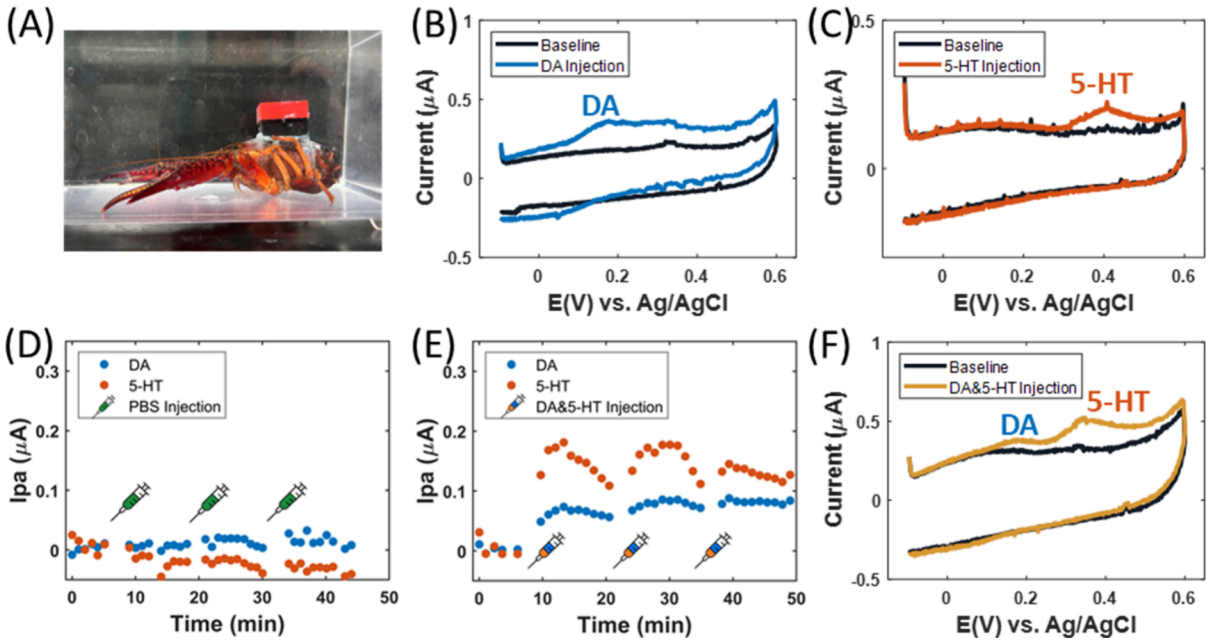

Figure 5. Simultaneous monitoring of DA and 5-HT in crayfish hemolymph. (A) Photograph of crayfish with the integrated electrochemical sensing device attached; (B) representative response currents before and after DA-only injection (0.5 mL of 3 mM); (C) representative response currents before and after 5-HT-only injection (0.5 mL of 3 mM); (D) background-subtracted Ipas after three PBS injections (0.5 mL each; negative control); (E) background-subtracted Ipas after three DA&5-HT cocktail injections (300 μM; 0.5 mL each); (F) representative response currents before and after DA&5-HT cocktail injection (0.5 mL of 300 μM).

both setups. Similarly, the cyclic voltammograms of 1 μM 5-HT show that the Epa was 0.43 V from VSP-300 and 0.32 V using our system (Figure 4C). The Ipas were measured as 122 and 118 nA for the benchtop and our system, respectively. While the comparison demonstrates that our sensing device had very similar Ipas, Epa was shifted to a lower potential. The constant potential peak shift is likely due to the difference in RE potentials between the commercial Ag/AgCl (3 M KCl) RE and our customized Ag/AgCl RE, which is verified in Figure S5.

CV responses of the electrochemical device to DA and 5-HT are shown in Figure 4D–F, and the sensitivities are calculated in Figure 4G–I. In Figure 4D, the voltammetric response of the device is shown for increasing DA concentration within the linear range of 0.1 to 1.2 μM, exhibiting a sensitivity of 95 nA/μM, with an LOD of 85.5 nM and a σ of 2.70 nA (Figure 4G). Figure 4E shows the voltammetric response of the electrochemical device for 5-HT detection, exhibiting a linear relationship in the range of 0.1 to 1 μM with a sensitivity of 159 nA/μM, with an LOD of 108.4 nM and a σ of 5.75 nA (Figure 4H). The electrochemical system was also tested for simultaneous detection of DA and 5-HT in the range of 0.1 to 1 μM, demonstrating a sensitivity of 48 nA/μM with an LOD of 152.4 nM (σ = 2.46 nA) for DA and a sensitivity of 133 nA/μM with an LOD of 51.6 nM (σ = 2.29 nA) for 5-HT, respectively (Figure 4F,I).

The physical characteristics and electrochemical performance of this wireless DA and 5-HT sensing system, in comparison with other reported devices, is summarized in Table S1.[37−40] Balancing between physical dimensions and electrochemical performance, our device utilizes CV techniques and has demonstrated the capability of detecting multiple neurotransmitters simultaneously with similar LODs compared to previously reported works. For example, the Wireless Instantaneous Neurotransmitter Concentration Sensing System (WINCS) was developed to monitor neurotransmitters in animals. Although both WINCS and our system rely on CFME as the transducer for detecting DA and 5-HT electrochemically, the WINCS system utilizes fast scan cyclic voltammetry (FSCV), while our device applies CV. FSCV inherently offers faster scan rates (>400 V/s) and can enhance antifouling properties, thereby improving time resolution. However, the limitation or disadvantage of FSCV is apparent: it is challenging to minimize and requires the capability to process large number data sets. As a result, the WINCS system, (130 × 84 × 47 mm),[40] is substantially larger in comparison to our device (28 × 23 × 21 mm). A compact footprint is essential for performing electrochemical measurements on freely moving animals. In contrast, the WINCS system has only been utilized in brain slices and anesthetized animals, not in live animals. Approximately 80% of the total weight of our device is attributed to the waterproof package and battery necessary for BLE communication. The use of BLE communication offers advantages over infrared (IR) communication; it does not require direct line-of-sight between devices, has a longer communication range, and can operate in more complex environments. Overall, our system is unique in its relatively small size, which is beneficial for monitoring both DA and 5-HT simultaneously in small animals.

***In Vivo* DA and 5-HT Detection in Crayfish with Integrated Electrochemical Sensing System.** The performance of the wireless electrochemical sensing system was further verified through the simultaneous *in vivo* detection of DA and 5-HT in crayfish. The device was attached to the crayfish carapace, with the electrodes implanted directly under the dorsal carapace into the heart to continuously monitor the response currents to DA and 5-HT in the crayfish hemolymph (Figure 5A). The total weight of the device was 7.8 g, which was designed to be neutrally buoyant and waterproof to minimize its impact on animal behavior in water.

https://doi.org/10.1021/acssensors.3c02304
ACS Sens. XXXX, XXX, XXX−XXX

It is common to study the function of neurotransmitters through injection for their roles of modulating different behaviors (or behavioral states), particularly the propensity for aggression during dyadic agonistic encounter as well as in the investigation of anxiety-like responses. For example, injection of 5-HT in socially subordinate crayfish hemolymph with an estimated final concentration of 10 μM was used to alter willingness of re-engage in further agonistic encounters with a socially dominant crayfish.[41] Similarly, 5 μg/g of 5-HT (equivalent to 1.7 mM of 0.5 mL) was injected into crayfish hemolymph to induce anxiety-like behaviors.[42] However, these work either did not monitor the dynamic of the injected neurotransmitter(s), or they were quantified with HPLC off-line.[43] Here, our device was the first to characterized "real-time", online internal detection of DA and/or 5-HT after single injection of DA solution (0.5 mL of 3 mM) and 5-HT solution (0.5 mL of 3 mM). Representative cyclic voltammograms before and after the DA injection event (Figure 5B) and 5-HT injection event (Figure 5C) clearly show oxidation peak for DA (0.18 V) and 5-HT (0.4 V), respectively.

To simulate an elevated concentration of DA and 5-HT near the electrode implantation site, which might occur during natural behaviors in crayfish, and to examine the device's capability for codetection in an *in vivo* environment, injections of 1× PBS (0.5 mL, as a negative control) and a DA&5-HT cocktail solution (0.5 mL of 300 μM) were administered, respectively, through the ventral sinus cavity of the crayfish and circulated through the heart.[21] During each experiment, five CV cycles were recorded, starting with the unaltered hemolymph (baseline), followed by three injection events. After each injection event, 10 cycles were continuously recorded, with a 1 min holding time between cycles. The monitoring results in crayfish are shown in Figure 5D−F. No change in Ipa was observed in the hemolymph measurements prior to any injections, and the administration of PBS did not result in an increase in Ipa at the DA or 5-HT potential (Figure 5D).

Representative cyclic voltammograms before and after a DA&5-HT cocktail injection event is shown in Figure 5F. No peaks were observed in the unaltered hemolymph, while two distinctive peaks were observed at 0.18 (DA) and 0.38 V (5-HT) following the DA&5-HT cocktail injection, which was consistent with the beaker-level characterization. Figure 5E summarizes the CV oxidation peaks resulting from the continuous monitoring of crayfish hemolymph, depicting the dynamics of DA and 5-HT levels before and after injection events. Immediately after the DA&5-HT cocktail injection, a clear increase in Ipa was observed, and the maximum measured Ipa reached 73.5 nA for DA and 181.1 nA for 5-HT 4 min after the injection. The Ipas decreased over time until the next injection event. A similar pattern was observed for the second and third injection events. For the second injection, the measured Ipa reached its maximum 5 min after injection, at 87.7 nA for DA and 177.3 nA for 5-HT. For the third injection, the maximum Ipas were 87.9 nA for DA and 145.1 nA for 5-HT. Overall, the Ipas are higher for 5-HT compared to DA, which is likely due to higher electrode sensitivity toward 5-HT than DA. The successive reduction in Ipas following the injection potentially occurred due to a combination of chemical metabolism,[44] dilution,[21] and possible fouling of CFME fibers due to long cycling. These findings demonstrate that the wireless neurotransmitter sensing system can successfully monitor the *in vivo* dynamics of injected 5-HT and DA in the hemolymph of freely behaving crayfish.

CONCLUSIONS

In conclusion, we have demonstrated a fully integrated untethered wireless electrochemical sensing device for the continuous monitoring of DA and 5-HT in hemolymph of freely behaving crayfish. This device utilizes surface-modified carbon fiber microelectrodes coupled with a miniaturized potentiostat module for wireless operation and data acquisition. The device exhibits high selectivity, sensitivity, and stability while maintaining a small footprint to minimize its impact on animal behavior. The integrated electrochemical sensing system enables detection of DA and 5-HT with a sensitivity of 48.4 and 133.0 nA/μM, respectively, within its submicromolar linear range. Furthermore, the successful *in vivo* measurements demonstrate the simultaneous monitoring of DA and 5-HT dynamics during injection events in freely behaving crayfish. Quantifying the absolute concentration of DA and 5-HT *in vivo* in crayfish could be beneficial when comparing between animals (e.g., during a dyadic agonistic encounter), but this remains challenging due to variations in the carapace curvature and the amount of hemolymph in the pericardial space, resulting in differences in the exposed area of the sensing region of the electrode tip to the circulating hemolymph. To address this issue, a potential solution could involve customizing the 3D package design to better suit the size of the crayfish and allow for an adjustable electrode implantation depth to ensure consistency.

Although this work has been focused on monitoring experimentally manipulated neurotransmitter dynamics, which can provide real-time analysis and information to study their behavioral effects, it also shows the potential to monitor endogenously released neurotransmitter dynamics induced by the level of aggressiveness and in the process of social status formation. Future work will focus on detecting endogenously released DA and 5-HT in the central nervous system (CNS) of crayfish, which have been shown to orchestrate a suite of social behaviors. This includes the initiation of fights, the decision that leads to discrete social status (i.e., dominance/subordinate), and the maintenance of such outcomes.[6,7,22,44−47] Due to the fast neurotransmitter transmission in the CNS, which lasts several hundreds of microseconds,[48] a faster electrochemical technique such as differential pulse voltammetry (DPV) can be implemented with the developed system. A modified DPV technique has been used to reduce the time of analysis to 1−2 s without losing selectivity.[49] Considering that DA and 5-HT are released locally in the CNS near dopaminergic neurons or serotonergic neurons, the implanted electrode may face a large concentration variation between DA and 5-HT depending on the implantation site, which may cause potential interferences. The use of small step sizes in DPV produces narrower voltammetric peaks, making it a preferred method for distinguishing analytes with similar oxidation potentials.[50] Additionally, the DA concentration can be determined from its reduction peak. A mathematical model can be built to estimate its oxidation peak and separate it from the overlapped oxidation peak to determine 5-HT concentrations.

Collectively, we envision that these advanced strategies provide a promising approach to tackle unresolved challenges related to neurohormonal DA and 5-HT associated with agonistic and nonagonistic behaviors and enable chronic

https://doi.org/10.1021/acssensors.3c02304
ACS Sens. XXXX, XXX, XXX−XXX

monitoring in crayfish and other aquatic (or terrestrial) animal species, potentially in their natural habitats (e.g., in a burrow or under a pond). This contribution could facilitate the investigation of fundamental neuromodulation research questions.

MATERIALS AND METHODS

Electrode Fabrication and Modification. The three-electrode electrochemical setup comprises a working electrode (WE) made of carbon fiber with a modified surface, a reference electrode (RE) consisting of Ag/AgCl, and a counter electrode (CE) made of Pt. The working electrode, referred to as Nafion-CNT/EC CFME, was constructed by utilizing T-650 carbon fibers from Solvay (Belgium) and modifying them using a solution containing Nafion and CNT. Additionally, electrochemical activation was employed to enhance the electrode's sensitivity. This procedure was slightly modified based on previously reported.[26] Before processing, multiple fibers were inserted into a glass capillary with an inner diameter of 0.4 mm (A-M Systems, WA). The carbon fiber was epoxied by dipping in 80 °C Epon 828 epoxy (Hexion, OH) and 14% m-phenylenediamine hardener (Sigma-Aldrich, MO) for 30 s to seal the fiber with the glass capillary, followed by dipping in acetone to remove excess epoxy on the tip area. Copper wire (30 AWG) was inserted into the glass capillary from the backside, providing electrical connections between the fiber strand and the electronics. The CFME was trimmed to a 5 mm tip and electrochemically treated via CV in phosphate buffered saline (1× PBS, containing 8g/L NaCl, 0.2 g/L KCl, 1.44 g/L Na_2HPO_4, and 0.24 g/L NaH_2PO_4, pH 7.4, Research Product International, IL) by applying a triangular wave from 0 to +2.5 V and 0 to −1.5 V at a scan rate of 100 mV/s. The fibers were then dip-coated in 0.5 mg/mL of single-walled CNT (P3-SWNT, Carbon Solutions, CA), dispersed in a 2.5% Nafion solution, and air-dried for 30 min before use. The Ag/AgCl RE was fabricated by electrodepositing AgCl onto a Ag wire (A-M Systems, WA) in 3 M KCl solution. A constant current bias of 0.15 mA was applied until a uniform AgCl coating was observed. The Pt wire CE was used as purchased (A-M Systems, WA).

Operation of Potentiostat Module. In our previous work,[51,52] a custom miniaturized potentiostat module and PCB was developed to perform wireless amperometric measurements. The flex-rigid PCB was fabricated and assembled by Sierra Circuits (Sunnyvale, CA) and comprises six layers, with components mounted onto two rigid ceramic (FR-4) substrates and connected via an embedded flex polyimide with 0.5 oz copper interconnects. The module combines an electrochemical analog-front end (AFE) IC (AD5941, Analog Devices, MA) and Bluetooth low energy microcontroller (BLE-MCU, BGM13S, Silicon Laboratories, TX) to control the sensor excitation voltages, capture and amplify the sensor signal, and transmit the data to a paired smartphone (Figure S1). Here, the system capabilities are extended to enable CV measurements of the Nafion-CNT/EC CFME and optimized for wireless *in vivo* detection of DA and 5-HT. MATLAB (MathWorks, MA) was utilized for data processing and visualization.

CV waveforms are generated based on user-defined measurement parameters such as step size, step duration, number of data points, ramp duration, and transimpedance amplifier (TIA) resistance. The excitation voltage sweep is produced by the digital-to-analog converter (DAC) in an iterative staircase-like manner closely resembling a linear analog voltage sweep. In this study, the CV waveform was produced with a potential range of −0.1 to +0.6 V, with other parameters optimized to enhance measurement sensitivity for the detection of DA and 5-HT. To accommodate hardware limitations, such as the minimum step size and step duration, a scan rate of 100 mV/s was used, resulting in a step size of 3.5 mV, a step duration of 35 ms, a ramp duration of 14 s, and 400 total recorded data points. The feedback resistance of the TIA was set to 512 kΩ to maximize measurement resolution, since the peak current was estimated to be below 1 μA during measurements. The waveform generated by the customized potentiostat module was verified using an oscilloscope (Tektronix, OR).

To extend the operational lifetime of the portable module, a magnetic reed switch was placed between the battery and voltage regulator such that when idle, the presence of a magnetic field would power off the device. When powered, the BLE-MCU polls to establish a connection and, once paired with a smartphone, via the EFR Connect Mobile App (Silicon Laboratories, TX), enters low-power mode and waits for a command. External commands are sent to the BLE-MCU to control the device's function. In this case, when the MCU is prompted to initiate the CV function, the AFE generates a triangular waveform for the microelectrode. The electrochemical oxidation current related to 5-HT concentration was converted to a measurable analog voltage signal using the TIA, digitized by the analog-to-digital converter (ADC), and stored in the AFE's internal memory until completing a full CV cycle. The MCU periodically samples the AFE (rate: 100 ms) using SPI to determine when data are available and then transmits the stored data via BLE to the external smartphone.

Surface Verification of the CFME. All SEM images and EDS analyses were acquired in the University of Maryland Nanocenter AIMlab using a Tescan GAIA (Czech Republic).

The electrochemical characterization of the bare and EC/Nafion-CNT CFME was conducted by EIS and CV measurements performed by the VSP-300 benchtop potentiostat (BioLogic, France) in 0.1 M KCl with 10 mM $[Fe(CN)_6]^{3-}/[Fe(CN)_6]^{4-}$ solution. The three-electrode system was used with a CFME as the WE, Ag/AgCl as RE (CH Instruments, TX), and Pt as CE (CH Instruments, TX). For the EIS measurements, the potential was set to 0 V and a frequency of 0.1 to 1 MHz. For the CV measurement, the potential ranges from −0.1 to 0.6 V with a scan rate of 100 mV/s.

Electrochemical Measurements of DA and 5-HT. DA (Sigma-Aldrich, MO) and 5-HT (Alfa Aesar, MA) stock solutions were diluted to different concentrations with 1× PBS for detection. The electrochemical measurements were performed using either the benchtop potentiostat VSP-300 with standard RE/CE or the PCB potentiostat module with customized RE/CE. CVs were obtained in the potential range from −0.2 to 0.6 V at a scan rate of 100 mV/s with a 1 min holding time between each measurement.

Simultaneous *In Vivo* Detection of DA and 5-HT. *In vivo* experimentation was carried out on wild-caught adult red swamp crayfish (*Procambarus clarkii*) purchased from a commercial supplier (Niles Biological, CA). Crayfish were housed in aquarium tanks in a 21 °C, 12 h/12 h light/dark cycle-controlled aquarium room and were fed *ad libitum* (an average of 2 pellets per animal) with formula one pellets (Ocean Nutrition, CA) twice a week. Crayfish with intact claws and no sign of body injury were anesthetized on ice for at least 15 min prior to surgery. Small incisions were then made through the dorsal carapace of the crayfish to expose the pericardial cavity, allowing direct implantation of electrodes into the heart. After the implant, there was a 15 to 20 min recovery period to allow the crayfish to "wake up" and allow the device to better adhere to crayfish's dorsal carapace of its thorax. Throughout CV cycling, the crayfish was fully awake and moving freely underwater. By injecting a drug into the ventral sinus cavity of crayfish, an animal with an open circulatory system, the drug enters the hemolymph, is being taken up by the heart and pumped into arteries. This allows detection of the drugs by the implanted electrode.

The device was glued onto the crayfish back above the surgery site, and electrodes were implanted in the crayfish for CV measurements. The potential ranged from −0.1 to 0.6 V with a scan rate of 100 mV/s and 1 min accumulation time. To test the system performance *in vivo*, the response currents of the crayfish hemolymph were initially recorded as the baseline. Then, the internal DA and 5-HT concentrations were changed by injecting the neurotransmitters into the animals, and the variations in the response currents were continuously recorded.

https://doi.org/10.1021/acssensors.3c02304
ACS Sens. XXXX, XXX, XXX−XXX

■ ASSOCIATED CONTENT

Supporting Information

The Supporting Information is available free of charge at https://pubs.acs.org/doi/10.1021/acssensors.3c02304.

Additional details on circuit design, source code, EDS analysis for microelectrodes, selectivity, and comparison to existing work (PDF)

■ AUTHOR INFORMATION

Corresponding Author

Reza Ghodssi − *Department of Electrical and Computer Engineering, University of Maryland, College Park, Maryland 20742, United States; Institute for Systems Research and Robert E. Fischell Institute for Biomedical Devices, University of Maryland, College Park, Maryland 20742, United States;* Email: ghodssi@umd.edu

Authors

Jinjing Han − *Department of Electrical and Computer Engineering, University of Maryland, College Park, Maryland 20742, United States; Institute for Systems Research and Robert E. Fischell Institute for Biomedical Devices, University of Maryland, College Park, Maryland 20742, United States;* orcid.org/0000-0001-6664-9839

Ta-wen Ho − *Department of Psychology and Program in Neuroscience and Cognitive Science, University of Maryland, College Park, Maryland 20742, United States;* orcid.org/0000-0003-0656-8214

Justin M. Stine − *Department of Electrical and Computer Engineering, University of Maryland, College Park, Maryland 20742, United States; Institute for Systems Research and Robert E. Fischell Institute for Biomedical Devices, University of Maryland, College Park, Maryland 20742, United States*

Sydney N. Overton − *Department of Electrical and Computer Engineering, University of Maryland, College Park, Maryland 20742, United States; Institute for Systems Research and Robert E. Fischell Institute for Biomedical Devices, University of Maryland, College Park, Maryland 20742, United States*

Jens Herberholz − *Department of Psychology and Program in Neuroscience and Cognitive Science, University of Maryland, College Park, Maryland 20742, United States*

Complete contact information is available at: https://pubs.acs.org/10.1021/acssensors.3c02304

Author Contributions

#J.H. and T.H. contributed equally to this paper

Notes

The authors declare no competing financial interest.

■ ACKNOWLEDGMENTS

The authors acknowledge financial support from the NSF (NCS #1926793). We thank the Maryland Nanocenter and the Advanced Imaging and Microscopy Laboratory (AIMlab) for their assistance in taking the SEM images.

■ REFERENCES

(1) Arias-Carrión, Ó.; Pöppel, E. Dopamine, Learning, and Reward-Seeking Behavior. *Acta Neurobiol Exp (Wars)* **2007**, *67* (4), 481−488.

(2) Baik, J. H. Dopamine Signaling in Reward-Related Behaviors. *Front. Neural Circuits* **2013**, *7*, 152 DOI: 10.3389/fncir.2013.00152.

(3) Barron, A. B.; Søvik, E.; Cornish, J. L. The Roles of Dopamine and Related Compounds in Reward-Seeking Behavior across Animal Phyla. *Front. Behav. Neurosci.* **2010**, *4*, 163.

(4) Bacqué-cazenave, J.; Bharatiya, R.; Barrière, G.; Delbecque, J. P.; Bouguiyoud, N.; Di Giovanni, G.; Cattaert, D.; De Deurwaerdère, P. Serotonin in Animal Cognition and Behavior. *Int. J. Mol. Sci.* **2020**, *21* (5), 1649.

(5) Edwards, D. H.; Herberholz, J. Crustacean Models of Aggression. In *Biology of Aggression*; Nelson, R. J., Ed.; Oxford University Press: New York, 2006; pp 38−62. DOI: 10.1093/acprof:oso/9780195168761.003.0003.

(6) Yamaguchi, Y.; Lee, Y. A.; Kato, A.; Jas, E.; Goto, Y. The Roles of Dopamine D2 Receptor in the Social Hierarchy of Rodents and Primates. *Sci. Rep* **2017**, *7* (1), 43348.

(7) Watanabe, N.; Yamamoto, M. Neural Mechanisms of Social Dominance. *Front Neurosci* **2015**, *9* (APR), 154.

(8) Kravitz, E. A. Serotonin and Aggression: Insights Gained from a Lobster Model System and Speculations on the Role of Amine Neurons in a Complex Behavior. *J. Comp Physiol A* **2000**, *186* (3), 221−238.

(9) Darvesh, A. S.; Carroll, R. T.; Geldenhuys, W. J.; Gudelsky, G. A.; Klein, J.; Meshul, C. K.; Van Der Schyf, C. J. In Vivo Brain Microdialysis: Advances in Neuropsychopharmacology and Drug Discovery. *Expert Opin Drug Discov* **2011**, *6* (2), 109−127.

(10) Westerink, B. H. C. Brain Microdialysis and Its Application for the Study of Animal Behaviour. *Behavioural Brain Research* **1995**, *70* (2), 103−124.

(11) Sabatini, B. L.; Tian, L. Imaging Neurotransmitter and Neuromodulator Dynamics In Vivo with Genetically Encoded Indicators. *Neuron* **2020**, *108* (1), 17−32.

(12) Leopold, A. V.; Shcherbakova, D. M.; Verkhusha, V. V. Fluorescent Biosensors for Neurotransmission and Neuromodulation: Engineering and Applications. *Front. Cell. Neurosci.* **2019**, *13*, 474 DOI: 10.3389/fncel.2019.00474.

(13) Rodeberg, N. T.; Sandberg, S. G.; Johnson, J. A.; Phillips, P. E. M.; Wightman, R. M. Hitchhiker's Guide to Voltammetry: Acute and Chronic Electrodes for in Vivo Fast-Scan Cyclic Voltammetry. *ACS Chem. Neurosci.* **2017**, *8* (2), 221−234.

(14) Xu, C.; Wu, F.; Yu, P.; Mao, L. In Vivo Electrochemical Sensors for Neurochemicals: Recent Update. *ACS Sens.* American Chemical Society December 27, **2019**; pp *4* 3102−3118. .

(15) Su, Y.; Bian, S.; Sawan, M. Real-Time: In Vivo Detection Techniques for Neurotransmitters: A Review. *Analyst* **2020**, *145* (19), 6193−6210.

(16) Robinson, J. E.; Coughlin, G. M.; Hori, A. M.; Cho, J. R.; Mackey, E. D.; Turan, Z.; Patriarchi, T.; Tian, L.; Gradinaru, V. Optical Dopamine Monitoring with DLight1 Reveals Mesolimbic Phenotypes in a Mouse Model of Neurofibromatosis Type 1. *Elife* **2019**, *8*, No. e48983, DOI: 10.7554/eLife.48983.

(17) Sun, F.; Zhou, J.; Dai, B.; Qian, T.; Zeng, J.; Li, X.; Zhuo, Y.; Zhang, Y.; Wang, Y.; Qian, C.; Tan, K.; Feng, J.; Dong, H.; Lin, D.; Cui, G.; Li, Y. Next-Generation GRAB Sensors for Monitoring Dopaminergic Activity in Vivo. *Nat. Methods* **2020**, *17* (11), 1156−1166.

(18) Zhou, B.; Fan, K.; Guo, J.; Feng, J.; Yang, C.; Li, Y.; Shi, S.; Kong, L. Plug-and-Play Fiber-Optic Sensors Based on Engineered Cells for Neurochemical Monitoring at High Specificity in Freely Moving Animals. *Sci. Adv.* **2023**, *9* (22), No. eadg0218.

(19) Wan, J.; Peng, W.; Li, X.; Qian, T.; Song, K.; Zeng, J.; Deng, F.; Hao, S.; Feng, J.; Zhang, P.; Zhang, Y.; Zou, J.; Pan, S.; Shin, M.; Venton, B. J.; Zhu, J. J.; Jing, M.; Xu, M.; Li, Y. A Genetically Encoded Sensor for Measuring Serotonin Dynamics. *Nat. Neurosci* **2021**, *24* (5), 746−752.

(20) Livingstone, M. S.; Harris-Warrick, R. M.; Kravitz, E. A. Serotonin and Octopamine Produce Opposite Postures in Lobsters. *Science* **1980**, *208* (4439), 76−79.

(21) Panksepp, J. B.; Yue, Z.; Drerup, C.; Huber, R. Amine Neurochemistry and Aggression in Crayfish. *Microsc Res. Tech* **2003**, *60* (3), 360−368.

(22) Huber, R.; Panksepp, J. B.; Yue, Z.; Delago, A.; Moore, P. Dynamic Interactions of Behavior and Amine Neurochemistry in Acquisition and Maintenance of Social Rank in Crayfish. *Brain Behav Evol* **2001**, *57* (5), 271−282.
(23) Fossat, P.; Bacqué-Cazenave, J.; De Deurwaerdère, P.; Delbecque, J. P.; Cattaert, D. Anxiety-like Behavior in Crayfish Is Controlled by Serotonin. *Science* **2014**, *344* (6189), 1293−1297.
(24) Ibuchi, K.; Nagayama, T. Opposing Effects of Dopamine on Agonistic Behaviour in Crayfish. *J. Exp. Biol.* **2021**, *224* (12), jeb242057 DOI: 10.1242/jeb.242057.
(25) Shiratori, C.; Suzuki, N.; Momohara, Y.; Shiraishi, K.; Aonuma, H.; Nagayama, T. Cyclic AMP-Regulated Opposing and Parallel Effects of Serotonin and Dopamine on Phototaxis in the Marmorkrebs (Marbled Crayfish). *European Journal of Neuroscience* **2017**, *46* (3), 1863−1874.
(26) Han, J.; Stine, J. M.; Chapin, A. A.; Ghodssi, R. A Portable Electrochemical Sensing Platform for Serotonin Detection Based on Surface-Modified Carbon Fiber Microelectrodes. *Analytical Methods* **2023**, *15* (9), 1096−1104.
(27) Baur, J. E.; Kristensen, E. W.; May, L. J.; Wiedemann, D. J.; Wightman, R. M. Fast-Scan Voltammetry of Biogenic Amines. *Anal. Chem.* **1988**, *60* (13), 1268−1272.
(28) Hashemi, P.; Dankoski, E. C.; Petrovic, J.; Keithley, R. B.; Wightman, R. M. Voltammetric Detection of 5-Hydroxytryptamine Release in the Rat Brain. *Anal. Chem.* **2009**, *81* (22), 9462−9471.
(29) Tavakolian-Ardakani, Z.; Hosu, O.; Cristea, C.; Mazloum-Ardakani, M.; Marrazza, G. Latest Trends in Electrochemical Sensors for Neurotransmitters: A Review. *Sensors (Switzerland)* **2019**, *19* (9), 2037.
(30) Demuru, S.; Deligianni, H. Surface PEDOT:Nafion Coatings for Enhanced Dopamine, Serotonin and Adenosine Sensing. *J. Electrochem. Soc.* **2017**, *164* (14), G129−G138.
(31) Weese, M. E.; Krevh, R. A.; Li, Y.; Alvarez, N. T.; Ross, A. E. Defect Sites Modulate Fouling Resistance on Carbon-Nanotube Fiber Electrodes. *ACS Sens* **2019**, *4* (4), 1001−1007.
(32) Han, J.; Stine, J. M.; Chapin, A. A.; Ho, T.; Pena-Flores, N.; Herberholz, J.; Ghodssi, R. A Wearable System for Electrochemical Sensing of Serotonin in Crayfish. In *Hilton Head Workshop 2022: A Solid-State, Sensors, Actuators, and Microsystems Workshop*; 2022.
(33) Han, J.; Ho, T.; Stine, J. M.; Straker, M. A.; Herberholz, J.; Ghodssi, R. Implantable Biosensor for Continuous Serotonin Detection in Freely Moving Crayfish. In *The 22nd International Conference on Solid-State Sensors, Actuators and Microsystems (Transducers 2023)*; 2023.
(34) Kashish; Gupta, S.; Dubey, S. K.; Prakash, R. Genosensor Based on a Nanostructured, Platinum-Modified Glassy Carbon Electrode for Listeria Detection. *Analytical Methods* **2015**, *7* (6), 2616−2622.
(35) Perrin, J. H.; Nelson, D. A. Competitive Binding of Two Drugs for a Single Binding Site on Albumin: A Circular Dichroic Study. *J. Pharm. Pharmacol.* **2011**, *25* (2), 125−130.
(36) Wang, Z.-X. An Exact Mathematical Expression for Describing Competitive Binding of Two Different Ligands to a Protein Molecule. *FEBS Lett.* **1995**, *360*, 111−114.
(37) Li, Y. T.; Wickens, J. R.; Huang, Y. L.; Pan, W. H. T.; Chen, F. Y. B.; Chen, J. J. J. Integrated Wireless Fast-Scan Cyclic Voltammetry Recording and Electrical Stimulation for Reward-Predictive Learning in Awake, Freely Moving Rats. *J. Neural Eng.* **2013**, *10* (4), No. 046007.
(38) Liu, C.; Zhao, Y.; Cai, X.; Xie, Y.; Wang, T.; Cheng, D.; Li, L.; Li, R.; Deng, Y.; Ding, H.; Lv, G.; Zhao, G.; Liu, L.; Zou, G.; Feng, M.; Sun, Q.; Yin, L.; Sheng, X. A Wireless, Implantable Optoelectrochemical Probe for Optogenetic Stimulation and Dopamine Detection. *Microsyst Nanoeng* **2020**, *6* (1), 64.
(39) Stuart, T.; Jeang, W. J.; Slivicki, R. A.; Brown, B. J.; Burton, A.; Brings, V. E.; Alarcón-Segovia, L. C.; Agyare, P.; Ruiz, S.; Tyree, A.; Pruitt, L.; Madhvapathy, S.; Niemiec, M.; Zhuang, J.; Krishnan, S.; Copits, B. A.; Rogers, J. A.; Gereau, R. W.; Samineni, V. K.; Bandodkar, A. J.; Gutruf, P. Wireless, Battery-Free Implants for Electrochemical Catecholamine Sensing and Optogenetic Stimulation. *ACS Nano* **2023**, *17* (1), 561−574.
(40) Lee, K. H.; Lujan, J. L.; Trevathan, J. K.; Ross, E. K.; Bartoletta, J. J.; Park, H. O.; Paek, S. B.; Nicolai, E. N.; Lee, J. H.; Min, H.-K.; Kimble, C. J.; Blaha, C. D.; Bennet, K. E. WINCS Harmoni: Closed-Loop Dynamic Neurochemical Control of Therapeutic Interventions. *Sci. Rep* **2017**, *7* (1), 46675.
(41) Huber, R.; Smith, K.; Delago, A.; Isaksson, K.; Kravitz, E. A. Serotonin and Aggressive Motivation in Crustaceans: Altering the Decision to Retreat. *Proc. Natl. Acad. Sci. U. S. A.* **1997**, *94* (11), 5939−5942.
(42) Fossat, P.; Bacqué-Cazenave, J.; De Deurwaerdère, P.; Delbecque, J. P.; Cattaert, D. Anxiety-like Behavior in Crayfish Is Controlled by Serotonin. *Science* **2014**, *344* (6189), 1293−1297.
(43) Fossat, P.; Bacqué-Cazenave, J.; De Deurwaerdère, P.; Cattaert, D.; Delbecque, J.-P. Serotonin, but Not Dopamine, Controls the Stress Response and Anxiety-like Behavior in the Crayfish Procambarus Clarkii. *J. Exp. Biol.* **2015**, 2745 DOI: 10.1242/jeb.120550.
(44) Huber, R.; Smith, K.; Delago, A.; Isaksson, K.; Kravitz, E. A. Serotonin and Aggressive Motivation in Crustaceans: Altering the Decision to Retreat. *Proc. Natl. Acad. Sci. U. S. A.* **1997**, *94* (11), 5939−5942.
(45) Summers, C. H.; Winberg, S. Interactions between the Neural Regulation of Stress and Aggression. *Journal of Experimental Biology* **2006**, *209* (23), 4581−4589.
(46) Sato, D.; Nagayama, T. Development of Agonistic Encounters in Dominance Hierarchy Formation in Juvenile Crayfish. *Journal of Experimental Biology* **2012**, *215* (7), 1210−1217.
(47) Jiménez-Morales, N.; Mendoza-Ángeles, K.; Porras-Villalobos, M.; Ibarra-Coronado, E.; Roldán-Roldán, G.; Hernández-Falcón, J. Who Is the Boss? Individual Recognition Memory and Social Hierarchy Formation in Crayfish. *Neurobiol Learn Mem* **2018**, *147*, 79−89.
(48) Barberis, A.; Petrini, E. M.; Mozrzymas, J. W. Impact of Synaptic Neurotransmitter Concentration Time Course on the Kinetics and Pharmacological Modulation of Inhibitory Synaptic Currents. *Front. Cell. Neurosci.* **2011**, *5*, 6 DOI: 10.3389/fncel.2011.00006.
(49) Crespi, F.; Möbius, C.; Neudeck, A. Short-Range Differential Pulse Voltammetry for Fast, Selective Analysis of Basal Levels of Cerebral Compounds in Vivo. *J. Neurosci Methods* **1993**, *50* (2), 225−235.
(50) Venton, B. J.; DiScenza, D. J. Voltammetry. In *Electrochemistry for Bioanalysis*; Elsevier, 2020; pp 27−50. DOI: 10.1016/B978-0-12-821203-5.00004-X.
(51) Stine, J. M.; Ruland, K. L.; Beardslee, L. A.; Levy, J. A.; Abianeh, H.; Botasini, S.; Pasricha, P. J.; Ghodssi, R. Miniaturized Capsule System Toward Real-Time Electrochemical Detection of H2S in the Gastrointestinal Tract. *Adv. Healthcare Mater*; 2024, *13*, 2302897.
(52) Stine, J. M. Mesoscale Embedded Sensor-Integrated Systems for Localized Biomedical Monitoring. Ph.D. Thesis, University of Maryland, 2023.

https://doi.org/10.1021/acssensors.3c02304
ACS Sens. XXXX, XXX, XXX−XXX